JOURNAL OF ENZYME INHIBITION AND MEDICINAL CHEMISTRY
2021, VOL. 36, NO. 1, 462–468
https://doi.org/10.1080/14756366.2020.1870456

Taylor & Francis
Taylor & Francis Group

SHORT COMMUNICATION

OPEN ACCESS Check for updates

RETRACTED ARTICLE: Thiophen urea derivatives as a new class of hepatitis C virus entry inhibitors

Hyung Chul Ryu[a]*, Marc Windisch[b]*, Jee Woong Lim[a], Inhee Choi[b], Eun Kyu Lee[c], Hye Hyun Yoo[c] and Tae Kon Kim[d]

[a]R&D Center, J2H Biotech, Suwon, Gyeonggi-do, Republic of Korea; [b]Medicinal Chemistry, Institut Pasteur Korea, Seongnam, Gyeonggi-do, Republic of Korea; [c]Institute of Pharmaceutical Science and Technology and College of Pharmacy, Hanyang University, Ansan, Gyeonggi-do, Republic of Korea; [d]College of Science and Engineering, Jungwon University, Geosan-gun, Chungbuk, Republic of Korea

ABSTRACT

To develop unique small-molecule inhibitors of hepatitis C virus (HCV), thiophen urea (TU) derivatives were synthesised and screened for HCV entry inhibitory activities. Among them, seven TU compounds exhibited portent anti-viral activities against genotypes 1/2 (EC_{50} < 30 nM) and subsequently, they were further investigated; based on the pharmacological, metabolic, pharmacokinetic, and safety profiles, **J2H-1701** was selected as the optimised lead compound as an HCV entry inhibitor. **J2H-1701** possesses effective multi-genotypic antiviral activity. The docking results suggested the potential interaction of **J2H-1701** with the HCV E2 glycoprotein. These results suggest that **J2H-1701** can be a potential candidate drug for the development of HCV entry inhibitors.

ARTICLE HISTORY
Received 7 July 2020
Revised 27 December 2020
Accepted 28 December 2020

KEYWORDS
Entry inhibitor; hepatitis C virus; small molecule; thiophen urea

1. Introduction

Approximately 200 million people worldwide are chronically infected with hepatitis C virus (HCV). This pathogen is the major cause of acute hepatitis and chronic liver disease, including cirrhosis and liver cancer[1]. HCV is an enveloped, positive-stranded RNA virus and a member of the Flaviviridae family in the hepacivirus genus. HCV is closely related to the *flavivirus* genus, which includes a number of viruses implicated in human disease, such as dengue virus and yellow fever virus[2]. Seven major HCV genotypes and numerous subtypes have been described and differ as much as 30% in nucleotide sequence[3,4].

Despite increasing efforts to develop novel drugs effective against HCV, patients are mainly being treated with a virus-unspecific combination therapy of pegylated interferon alpha (PEG-IFN) and ribavirin[5,6]. This treatment is expensive and can be associated with severe side effects; in addition, it is effective in only 50–60% of patients infected with HCV genotype 1[7]. Since early 2011, two direct acting antivirals (DAAs) targeting the viral NS3 protease have been approved by the United States Food and Drug Administration. Unfortunately, both drugs induce severe side effects and have a low resistance barrier as well as an inconvenient administration regime[8]. Viral resistance may eventually become an issue; due to potential HCV genotype specificity, it is unclear whether all seven HCV genotypes and their subtypes are covered[9]. Therefore, it is a primary goal to identify targets with a significantly higher genetic barrier of resistance that cover all HCV genotypes. Other challenges include appearance of escape mutants, high costs of current therapy regimens, and negative side effects. The mechanisms of resistance to interferon (IFN)-based therapy through immune system interception[10] and also to DAAs like telaprevir and boceprevir through resistance-conferring mutations could be avoided by combinatorial treatment. Although drugs that target the virus are currently in clinical trials, a medical need remains for new HCV therapeutic agents. There is a particular need for HCV therapeutic agents that have broad activity against the majority of HCV genotypes and their subtypes (e.g. 1a/b, 2a/b 3a/b, 4a/b, etc.).

The entry process of HCV into hepatocytes has been recognised as one of the potential targets for therapeutic intervention to treat or prevent HCV infection. To develop new types of small-molecule inhibitors for HCV, we first sought to screen HCV entry inhibitory molecules using an infectious cell culture system (HCVcc). During the preliminary screening[11], thiophen urea (TU) derivatives were found to possess useful activity against all major HCV genotypes. Accordingly, we further tested 296 TU derivatives to determine the lead optimisation process. Herein, we present a new class of compounds that exert antiviral activity against HCV.

2. Experimental

2.1. General procedure for synthesis of TU derivatives

The target products were prepared in three steps as follows (Scheme 1).

1. Pyridine (190.23 mmol) and 4-nitrophenyl chloroformate (104.62 mmol) were added to a stirred solution of alkyl 2-amino-4,5-dialkylthiophene-3-carboxylate (**1**, 95.11 mmol) in

CONTACT Tae Kon Kim tkkim@jwu.ac.kr College of Science and Engineering, Jungwon University, Geosan-gun, Chungbuk, 367-700, Republic of Korea; Hye Hyun Yoo yoohh@hanyang.ac.kr Institute of Pharmaceutical Science and Technology and College of Pharmacy, Hanyang University, Ansan, Gyeonggi-do, 15588, Republic of Korea
*These authors contributed equally to this work.

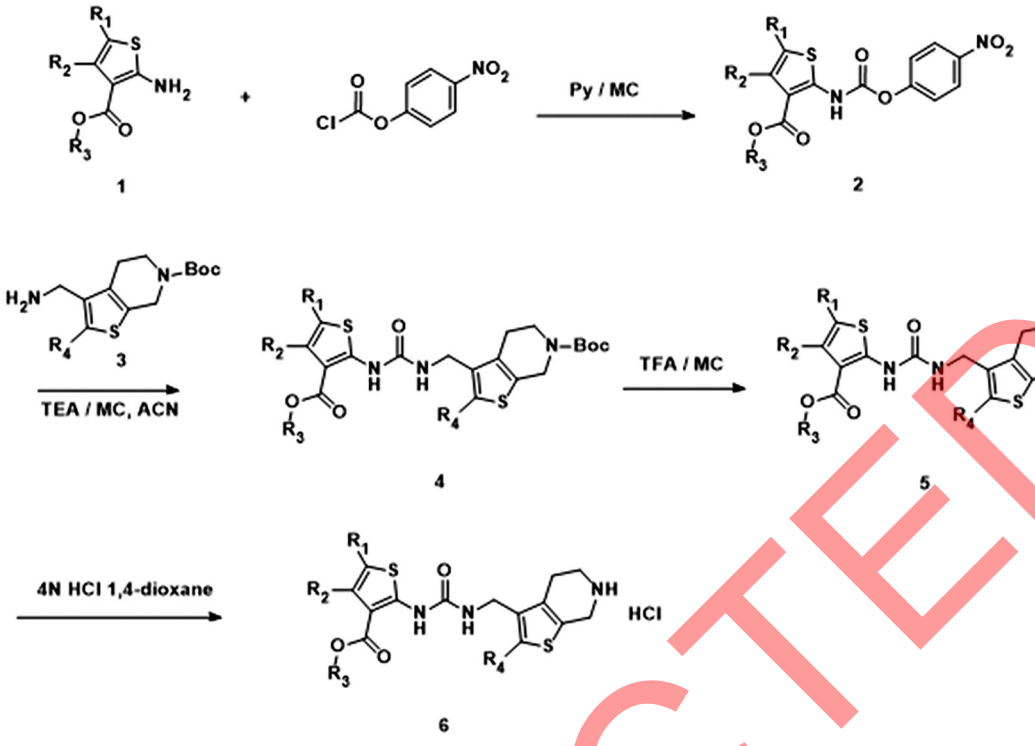

	R1	R2	R3	R4
J2H-1701			tert-butyl	CF_3
HCV-2577			Itert-butyl	4-F-Ph
HCV-2602			isopropyl	CF_3
HCV-2614			tert-butyl	3-Cl-Ph
HCV-2694	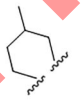		tert-butyl	CF_3
HCV-3149			isopropyl	CF_3
HCV-3083	ethyl	methyl	tert-butyl	CF_3

Scheme 1. Synthesis of TU derivatives.

anhydrous CH_2Cl_2 at 0 °C. The reaction mixture was warmed to room temperature and stirred for 2 h. After the reaction was completed, the reaction mixture was quenched with H_2O and extracted using CH_2Cl_2. The organic layer was dried over anhydrous $MgSO_4$, filtered, and concentrated. The crude product was precipitated by adding diethyl ether and kept at 4 °C for few hours to complete the precipitation. The precipitate was filtered and washed with diethyl ether and dried in vacuum to produce a 4-nitrophenoxycarbonylamino derivative (**2**) as a yellow solid.

2. A solution of the above intermediate (**2**, 56 mmol), *tert*-butyl 3-(aminomethyl)-2-*R*-substituted-4,7-dihydrothieno[2,3-*c*]pyridine-6(5*H*)-carboxylate (**3**, 62 mmol), and triethylamine (113 mmol) in CH_2Cl_2 was stirred overnight at room temperature. The organic solution was washed with H_2O, dried over anhydrous $MgSO_4$, and concentrated under reduced pressure. The solid product was filtered and washed with diethyl ether to obtain a pure compound (**4**) as a pale yellow solid.
3. Trifluoroacetic acid (155.9 mmol) was added to a stirred solution of the above intermediate (**4**, 19.4 mmol) in CH_2Cl_2 at

0 °C. The reaction mixture was stirred at room temperature for 5 h. After the reaction was complete, the mixture was diluted with CH_2Cl_2 and washed with brine (br). Next, 2N NaOH (aq.) was slowly added to the separated organic solution at 10 °C, and then the suspension was stirred for 1.5 h. The precipitate was filtered and agitated with methyl *tert*-butyl ether for 2 h. The solid was filtered and washed with diethyl ether and dried under vacuum to obtain the product (**5**) as a white powder. The final product (6) could be obtained as an organic or inorganic salt by further process to get more stable solid state.

2.1.1. tert-butyl 2–(3-((2-(trifluoromethyl)-4,5,6,7-tetrahydrothieno[2,3-c]pyridin-3-yl)methyl)ureido)-4,5,6,7-tetrahydrobenzo[b]thiophene-3-carboxylate hydrochloride (J2H-1701)

White solid: ^{1}H NMR (400 MHz, $(CD_3)_2SO$) δ 10.37 (s, 1H), 9.23 (bs, 2 H), 8.26 (t, $J = 5.2$ Hz, 1H), 4.39 (s, 2H), 4.35 (d, $J = 4.8$ Hz, 2H), 3.39–3.38 (m, 2H), 2.92–2.84 (m, 2H), 2.64–2.59 (m, 2H), 1.74–1.62 (m, 4H), 1.51 (s, 9H); ^{13}C NMR (101 MHz, $(CD_3)_2SO$) δ 165.00, 153.38, 149.72, 139.61 (q, $J = 2.9$ Hz), 134.64, 131.05, 129.69, 124.42 (q, $J = 35.7$ Hz), 123.75, 122.74 (q, $J = 269.8$ Hz), 109.50, 80.56, 41.25, 39.89, 34.39, 28.03, 26.27, 23.70, 22.61, 22.54, 21.08; LCMS (electrospray) *m/z* $(M + H)^+$ 516.02.

2.1.2. tert-butyl 2–(3-((2–(4-fluorophenyl)-4,5,6,7-tetrahydrothieno[2,3-c]pyridin-3-yl)methyl)ureido)-4,5,6,7-tetrahydrobenzo[b]thiophene-3-carboxylate (HCV-2577)

White solid: ^{1}H NMR (400 MHz, $CDCl_3$) δ 10.65 (s, 1H), 7.38–7.30 (m, 2H), 7.12–7.04 (m, 2H), 4.76 (t, $J = 4.7$ Hz, 1H), 4.36 (d, $J = 4.9$ Hz, 2H), 4.01 (s, 2H), 3.12 (t, $J = 5.8$ Hz, 2H), 2.73–2.65 (m, 2H), 2.64–2.53 (m,4H), 1.83–1.69 (m, 4H), 1.52 (s, 9H); LCMS (electrospray) *m/z* $(M + H)^+$ 542.08.

2.1.3. tert-butyl 2–(3-((2–(3-chlorophenyl)-4,5,6,7-tetrahydrothieno[2,3-c]pyridin-3-yl)methyl)ureido)-4,5,6,7-tetrahydrobenzo[b]thiophene-3-carboxylate (HCV-2614)

White solid; ^{1}H NMR (400 MHz, $(CD_3)_2SO$) δ 10.34 (s, 1H), 8.10 (s, 1H), 7.56–7.35 (m, 4H), 4.15 (d, $J = 4.5$ Hz, 2H), 3.95 (s, 2H), 3.06–2.95 (m, 2H), 2.63 (s, 2H), 2.55 (s, 4H), 1.67 (s, 4H), 1.50 (s, 9H); LCMS (electrospray) *m/z* $(M + H)^+$ 558.07.

2.1.4. Isopropyl 2–(3-((2-(trifluoromethyl)-4,5,6,7-tetrahydrothieno[2,3-c]pyridin-3-yl)methyl)ureido)-4,5,6,7-tetrahydrobenzo[b]thiophene-3-carboxylate (HCV-2602)

White solid: ^{1}H NMR (400 MHz, $(CD_3)_2SO$) δ 10.36 (s, 1H), 8.14 (t, $J = 5.0$ Hz, 1H), 5.05 (quintet, $J = 6.4$ and 12.4 Hz, 1H), 4.30 (d, $J = 4.8$ Hz, 2H), 3.87 (s, 2H), 2.91 (t, $J = 5.8$ Hz, 2H), 2.66 (s, 2H), 2.53 (s, 4H), 1.69 (s, 4H), 1.29 (s, 3H), 1.27 (s, 3H); LCMS (electrospray) *m/z* $(M + H)^+$ 501.95.

2.1.5. tert-butyl 6-methyl-2–(3-((2-(trifluoromethyl)-4,5,6,7-tetrahydrothieno[2,3-c]pyridin-3-yl)methyl)ureido)-4,5,6,7-tetrahydrobenzo[b]thiophene-3-carboxylate (HCV-2694)

White solid: ^{1}H NMR (400 MHz, $(CD_3)_2SO$) δ 10.62 (s, 1H), 4.94 (bs, 1H), 4.48 (d, $J = 5.6$ Hz, 2H), 4.11 (s, 2H), 3.17 (t, $J = 6.0$ Hz, 2H), 2.87–2.83 (m, 2H), 2.78–2.75 (m, 2H), 2.69–2.59 (m, 2H), 2.24–2.18 (m, 1H), 1.86–1.83 (m, 2H), 1.53 (s, 9H), 1.38–1.32 (m, 1H), 1.05 (d, $J = 6.4$ Hz, 3H); LCMS (electrospray) *m/z* $(M + H)^+$ 530.11.

2.1.6. tert-butyl 5-ethyl-4-methyl-2–(3-((2-(trifluoromethyl)-4,5,6,7-tetrahydrothieno[2,3-c]pyridin-3-yl)methyl)ureido)thiophene-3-carboxylate (HCV-3083)

White solid: ^{1}H NMR (400 MHz, $(CD_3)_2SO$) δ 10.68 (s, 1H), 4.98 (bs, 1H), 4.49 (d, $J = 5.2$ Hz, 2H), 4.07 (s, 2H), 3.15 (t, $J = 5.6$ Hz, 2H), 2.73 (bs, 2H), 2.64 (q, $J = 7.2$ Hz, $J = 7.6$ Hz, 4H), 2.19 (s, 3H), 1.54 (s, 9H), 1.20 (t, $J = 7.6$ Hz, 3H); LCMS (electrospray) *m/z* $(M + H)^+$ 504.26.

2.1.7. Ethyl 2–(3-((6–(2-(dimethylamino)ethyl)-2-(trifluoromethyl)-4,5,6,7-tetrahydrothieno[2,3-c]pyridin-3-yl)methyl)ureido)-4,5,6,7-tetrahydrobenzo[b]thiophene-3-carboxylate dihydrochloride (HCV-3149)

Ivory solid: ^{1}H NMR (400 MHz, $(CD_3)_2SO$) δ 11.39 (bs, 1H), 10.64 (bs, 1H), 10.33 (s, 1H), 8.32 (s, 1H), 4.36 (bs, 2H), 4.24 (t, $J = 7.2$ Hz, 2H), 3.65–3.30 (m, 8H), 3.00 (s, 2H), 2.85 (s, 6H), 2.66 (s, 2H), 2.53 (s, 2H), 1.69 (bs, 4H), 1.28 (t, $J = 7.2$ Hz, 3H); LCMS (electrospray) *m/z* $(M + H)^+$ 559.40.

2.2. Genotype 1/2 chimeric HCVcc assay

Naïve Huh-7.5 target cells were plated at a concentration of 2400 cells/well in 25 μL of culture media in 384-well plates (Greinerbio: one, u clear black). After overnight incubation, compounds serially diluted in 10 μl of cell culture media were added. After 2 h of compound treatment, cells were inoculated with 40 μl of genotype 1/2 chimeric HCVcc, which expresses structural proteins of HCV genotype 1a isolate (TN accession number: EF621489) and non-structural proteins of HCV genotype 2a (JFH-1) with a nano-luciferase reporter. At 72 h post-infection, nano-luciferase activity (Nano: GloTM, Promega, Madison, WI) and cellular adenosine triphosphate (ATP; Cell titre: GloTM, Promega, Madison, WI) levels were measured as a marker of HCV replication and cytotoxicity, respectively. EC_{50} and CC_{50} were calculated by non-linear regression analysis using GraphPad Prism (GraphPad Software, La Jolla, CA).

2.3. Cross-genotypic antiviral activity

To evaluate cross-genotypic antiviral activity against various HCV genotypes, **J2H-1701** were tested using chimeric HCVcc as described above. HCV chimaeras expressing the structural proteins of HCV genotypes 1a (H77), 1 b (J4), 2a (E2P7), 2 b (J8), 3a (S52), 4a (ED43), 5a (SA13), 6a (HK6a), or 7a (QC69), followed by HCV genotype 2a (JFH-1)-derived non-structural proteins responsible for viral RNA replication and the Renilla luciferase reporter gene were used to monitor viral replication.

2.4. Molecular docking analysis

The HCV (genotype: 1a strain H77) E2 X-ray diffraction structure was obtained from the Protein Data Bank (PDB: 4MWF)[12]. Of the two enveloped glycoprotein E2 chains that are involved, chain D was selected for docking as its secondary structure was well-defined compared to chain C. The residues of T542RPPLG547 were not missing from this chain. The selected D chain of glycoprotein E2 was prepared for docking using the Protein Preparation tool. Molecular docking was carried out with Glide[13]. All possible binding pockets were analysed according to the binding cavities of the protein as well as the biologically meaningful regions. Four grids were generated for each assigned binding site, and the prepared three-dimensional ligand conformation of **J2H-1701** was

docked at each site. The best docked pose was determined based on the highest docking score and also any favourable interactions with the targeted residues. The selected docked complex was energy minimised with MacroModel using OPLS_2005 force field in a water environment (until converging at a termination gradient of 0.0001 kJ/mol Å) referring to the report by Di Maio et al.[14].

3. Results and discussion

Thiophen urea derivatives were synthesised in three steps as follows: a reaction of 4-nitrophenyl chloroformate, urea synthesis by amine substitution, and final deprotection (Scheme 1). In each step all products were easily obtained as a pure solid by a simple work-up method (precipitation or filtration) without further purification. Two starting materials that have a thiophen ring with various substituents were utilised to achieve structural diversity. Several compounds including **J2H-1701**, **HCV-2602**, and **HCV-2694** were prepared as an acid salt to enhance aqueous solubility using an additional method. For example, J2H-1701 was prepared as a HCl salt by treatment of HCl solution in 1,4-dioxane. Almost all the test compounds showed good chemical stability and crystallinity. **J2H-1701**, a representative compound as a HCl salt, has a long-term stability (purity >98% for 3 months) at room temperature, and so do the other compounds. This stability is supposed to come from its crystallinity that would be intrinsic property of thiophen urea structure, based on their high melting point and differential scanning calorimetry data (data not shown). When the drug-like properties of TU derivatives were assessed by Lipinski's rule of five[15], most of the compounds were shown to be applicable for orally available drugs; for example, J2H-1701, it has 3 hydrogen bond donors, 6 hydrogen bond acceptors, logP (experimental) of 4.21, and molecular weight of 515.62 and the number of violation is 1. Therefore, J2H-1701 is considered as an orally available drug.

Initially, we screened 296 TU derivatives for anti-viral activity against genotypes 1/2 using the infectious HCVcc system and seven selected compounds with potent activities for further *in vitro* ADME/toxicity studies (Figure 1, Table 1). Accordingly, *in vitro* ADME and cytotoxicity evaluations were conducted for the seven compounds to select the best potential drug candidate (Table 2). The compounds showed good metabolic stability in mouse and human liver microsomes, and they also were found to be stable in mouse and human plasma. In addition, the compounds did not reveal any negligible effects for CYP3A4 and CYP2A9 inhibition. However, some compounds showed significant cytotoxicity with human cell lines, including HEK293 (embryonic kidney cells), SK-N-SH (neuroblastomas), HepG2 (hepatomas), and Jurkat (immortalised T lymphocytes) (data not shown). Accordingly, based on these *in vitro* test results, **J2H-1701** was selected for further characterisation as an anti-HCV drug candidate.

J2H-1701 was tested for cross-genotype activities against seven genosubtypes (nine subtypes) of the virus using a dose–response assay in the HCVcc system. The representative dose–response plots for HCV inhibition and cytotoxicity are provided in Figure 2. **J2H-1701** generally exhibited potent inhibition against the six HCV genotypes (HCV genotype **1a**, **2a**, **2 b**, **3a**, **4a**, and **7a**) whereas no significant cytotoxicity was observed for all tested genosubtypes. **J2H-1701** showed IC_{50} values in the nano-subnanomolar range in several HCV subgenotypes, which is much lower than those of a well-known HCV inhibitor, sofosbuvir (Table 3). This demonstrates that **J2H-1701** possesses effective multi-genotypic antiviral activity.

Table 1. Anti-viral activities of the seven selected TU derivatives ($n = 2$).

	EC_{50} (cc GT1a/2a)	EC_{50} (cc GT2a)
J2H-1701	0.95 nM	10.9 nM
HCV-2577	5.0 nM	27.0 nM
HCV-2602	0.04 nM	1.1 nM
HCV-2614	0.5 nM	4.0 nM
HCV-2694	0.8 nM	1.7 nM
HCV-3083	2.6 nM	17.8 nM
HCV-3149	0.5 nM	2.1 nM

Table 2. *In vitro* pharmacokinetic properties of the seven selected TU derivatives ($n = 2$).

	Metabolic Stability[a] ($t_{1/2}$, min)	Plasma stability[b] (% after 4 h)	PAMPA permeability[c] (Log Pe, cm/s)	CYP3A4 IC_{50}[d] (μM)	CYP2C9 IC_{50}[e] (μM)
J2H-1701	>60	86.8	−5.95	>100	>100
HCV-2577	>60	91.5	ND	>10	>40
HCV-2602	>60	67.0	−7.44	>10	>40
HCV-2614	>60	110	−6.95	>10	>40
HCV-2694	>60	131	−8.26	>10	>40
HCV-3083	>60	86.9	−5.90	6.79	>10
HCV-3149	>60	97.2	−5.17	7.42	>10

[a]Metabolic stability in human liver microsomes at 1 μM. LC-MS/MS detection.
[b]Stability in human plasma at 1 μM. LC-MS/MS detection.
[c]Compound permeability measured using parallel artificial membrane permeability assay at 1 μM. LC-MS/MS detection.
[d,e]Measured using CYP specific probe substrates in human liver microsomes. LC-MS/MS detection.

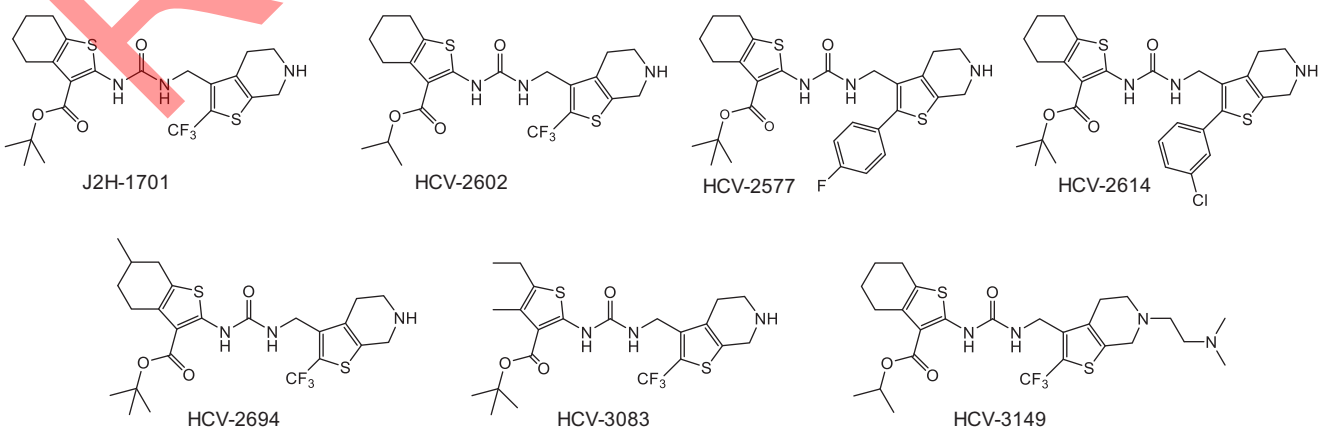

Figure 1. Chemical structures of the seven selected TU derivatives.

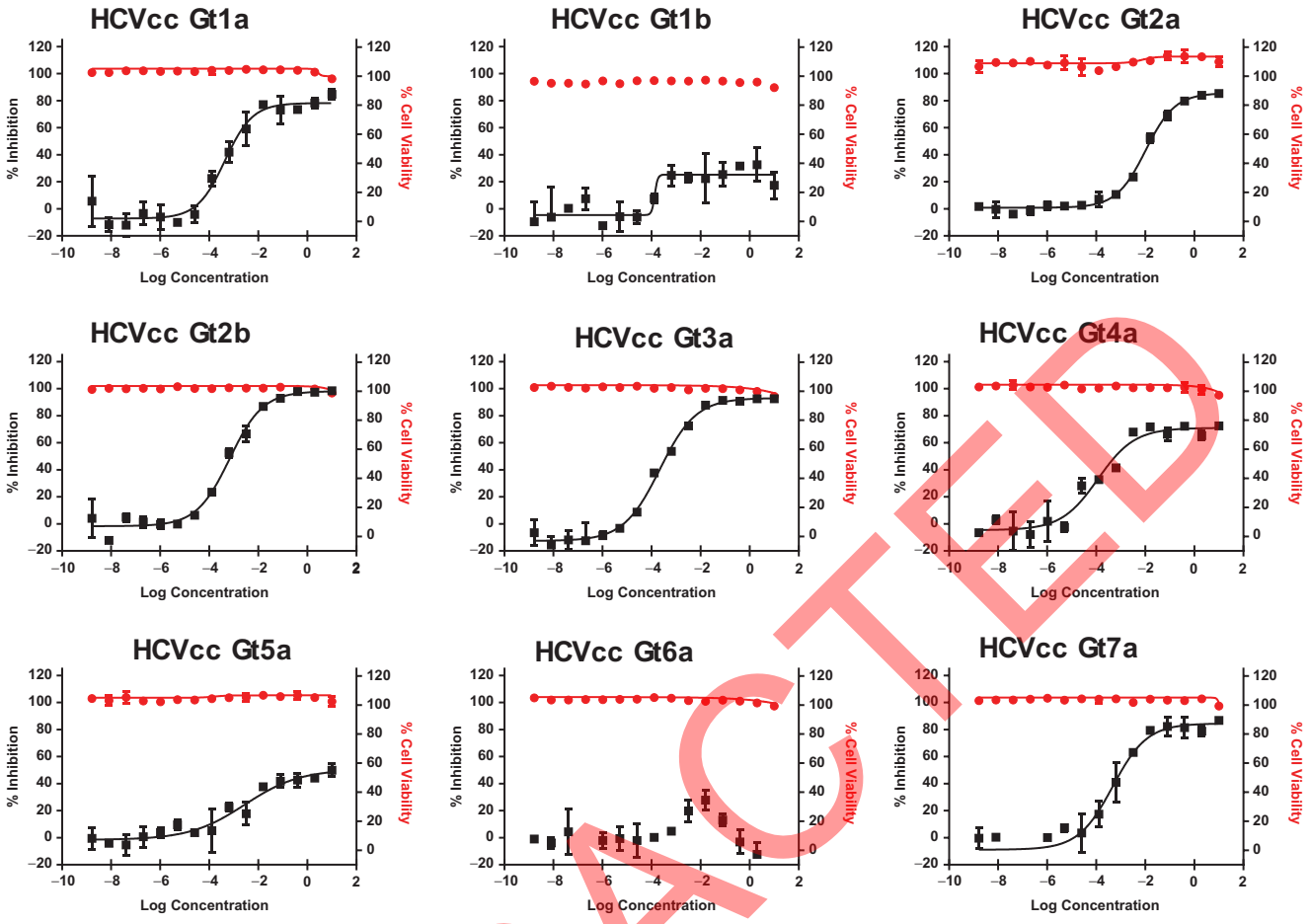

Figure 2. Cross-genotypic antiviral activity of **J2H-1701**.

Table 3. Cross-genotypic anti-HCV activities of J2H-1701 ($n = 3$).

	J2H-1701		Sofosbuvir	
	EC_{50} (nM)	CC_{50} (nM)	EC_{50} (nM)	CC_{50} (nM)
GT 1a	0.43	>10,000	173	>10,000
GT 1 b	na[a]	>10,000	814	>10,000
GT 2a	10	>10,000	159	>10,000
GT 2 b	0.68	>10,000	87	>10,000
GT 3a	0.21	>10,000	691	>10,000
GT 4a	3.2	>10,000	209	>10,000
GT 5a	~10,000	>10,000	672	>10,000
GT 6a	na	>10,000	366	>10,000
GT 7a	0.4	>10,000	2,594	>10,000

[a]Not available.

Since **J2H-1701** was shown to be an HCV entry inhibitor, we investigated the relevant mechanisms for HCV entry inhibition and found that **J2H-1701** inhibits HCV envelope proteins (data not shown). Accordingly, the HCV envelope glycoproteins were selected as a target protein for docking studies and we performed a molecular docking analysis on the crystal structures of the HCV E2 glycoprotein[12] to predict whether **J2H-1701** would interact with E1/E2 viral glycoproteins. Out of the four potential binding sites of the E2 monomer, **J2H-1701** fit snugly into the binding site (Figure 3(A)). This site is located in the loop region and is also a surface on the β sandwich of the E2 glycoprotein (Figure 3(B)), which has been identified by the mutagenesis study as being involved in interacting with CD81[12]. The interactions of **J2H-1701** with the residues of the E2 monomer indicated strong binding of **J2H-1701** within the E2 monomer. There were four hydrogen (H) bonds: 1) two H bonds formed with both nitrogens in the urea group and Val515; 2) one bond was made between the oxygen of the urea group and His421; and 3) another H bond formed with the nitrogen in piperidine and Thr425. The trifluoro group was docked around the threonines and valines in the β5 region of the β sandwich. The van der Waals interactions of the trimethyl group were observed with Thr510, Asn548, and Trp549 of the β sandwich (Figure 3(C)). The docking energy was −4.437 kcal/mol, which was the lowest among all docked poses. The docking score (GlideScore) was −4.437 kcal/mol, which was the lowest among all docked poses. The minimisation energy difference between the unbound protein structure (−28224.178 kJ/mol) and the **J2H-1701** docked structure (−28598.234) was −374.056 kJ/mol.

The docked site of **J2H-1701** has been reported to participate in CD81 receptor binding and also viral entry[12]. Recently, docking studies with berberine showed that it may potentially bind to the site on the E2 glycoprotein[16,17]. This site is located in the back layer of E2, which is about 11 Å away from the front layer – an area reported to participate in CD81 receptor binding and viral entry. **J2H-1701** demonstrated weaker docking activity to the back layer of the E2 glycoprotein (data not shown). Overall, the binding pose of **J2H-1701**, which favourably interacts with those residues known to participate in CD81 receptor binding and viral entry, indicates that **J2H-1701** most likely interacts with the HCV envelope glycoprotein E2.

The essential players in HCV virus entry are HCV glycoproteins E1 and E2, which form a heterodimer and constitute viral envelope proteins[18–20]. HCV E1 does not directly interact with host receptors, whereas E2 directly binds with host receptors, such as the CD81 receptor[21]. Therefore, we propose that **J2H-1701** would

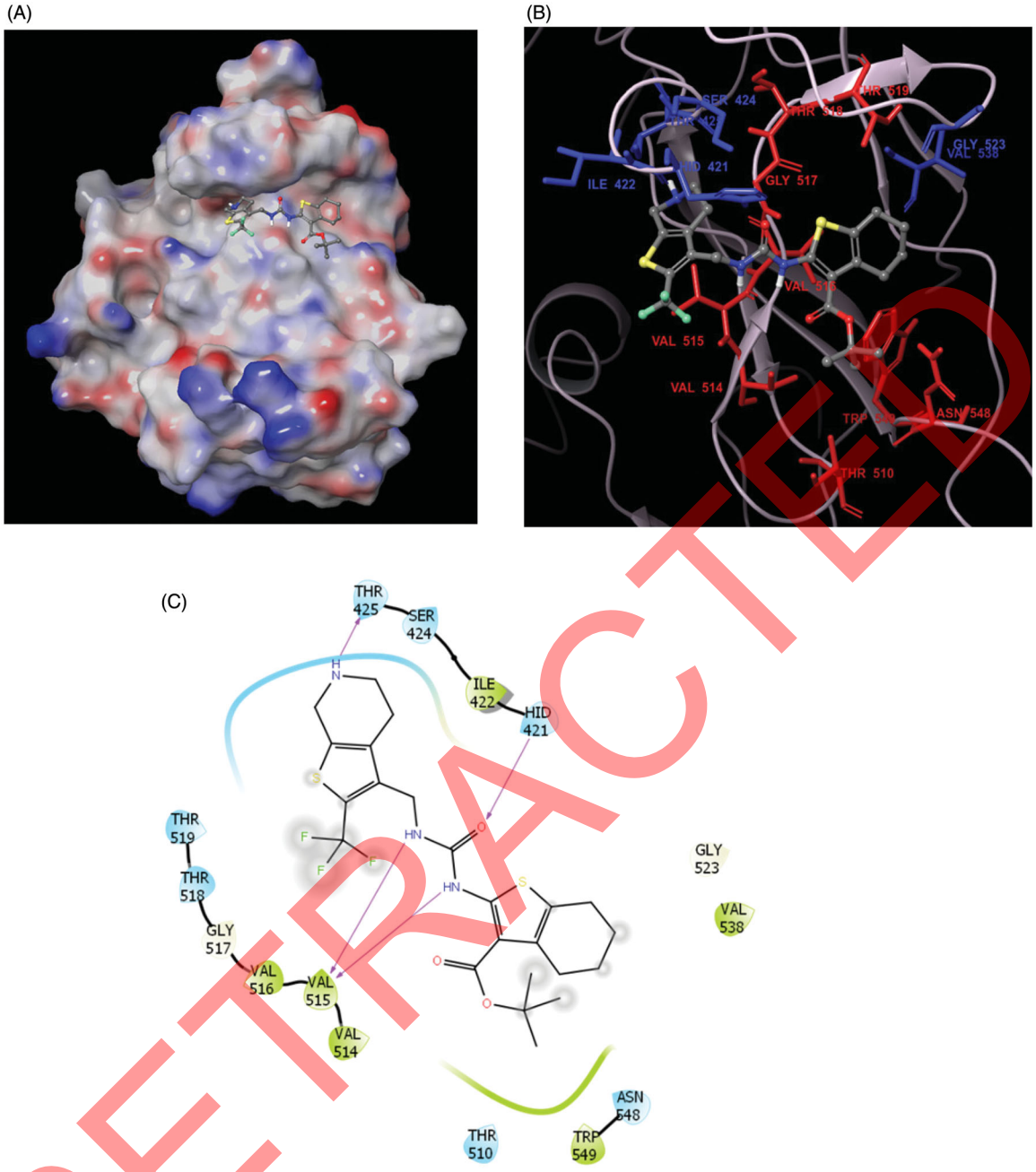

Figure 3. The molecular docking analysis of **J2H-1701**'s interaction with HCV E2. (A) The putative binding site of **J2H-1701** in the HCV E2 monomer. The E2 monomer is displayed as an electrostatic surface. **J2H-1701** is depicted using an atom-coloured ball-and-stick model. (B) **J2H-1701** is docked in the CD81 interacting sites of the E2 monomer, which are a surface on the β sandwich and the CD81 binding loop. Interacting residues from the β sandwich and the CD81 binding loop are coloured in red and blue, respectively. All residues are shown using a stick model and labelled appropriately. **J2H-1701** is displayed with an atom-coloured ball-and-stick model. (C) The ligand interaction diagram of **J2H-1701**. Solid magenta arrows indicate hydrogen bonds. All residues are labelled using coloured circles based on their side chains.

bind to E2 in order to neutralise CD81 receptor interaction and viral entry. The flexible conformation of compound **J2H-1701** demonstrated energetically favourable interactions with those targeted residues of E2 involved in the interaction of the CD81 receptor (mainly the loop) and the surface of the β sandwich.

4. Conclusions

In this study, TU derivatives were synthesised and tested for their potential as HCV entry inhibitors. The seven selected TU compounds exhibited potent anti-viral activities against genotypes 1/2 with EC_{50} values ranging from 0.04 to 27 nM. The compounds also showed good pharmacokinetic properties. However, some compounds significant cytotoxicity; accordingly, **J2H-1701** was selected as a potential anti-HCV drug candidate. The **J2H-1701** possesses effective multi-genotypic antiviral activity. The docking analysis results suggest that **J2H-1701** would bind to E2 to inhibit the entry of HCV. These results demonstrate that **J2H-1701** can be a potential candidate drug for the development of HCV entry inhibitors.

Acknowledgements

The authors thank Dr. Jason Kim in J2H biotech for supervision of structure activity relationship of medicinal chemistry.

Disclosure statement

No potential conflict of interest was reported by the author(s).

References

1. Lavanchy D. The global burden of hepatitis C. Liver Int 2009; 29:74–81.
2. Lindenbach BD, Rice CM. Unravelling hepatitis C virus replication from genome to function. Nature 2005;436:933–8.
3. Van Regenmortel MH. Virus species and virus identification: past and current controversies. Infect Genet Evol 2007;7: 133–44.
4. Simmonds P, Bukh J, Combet C, et al. Consensus proposals for a unified system of nomenclature of hepatitis C virus genotypes. Hepatology 2005;42:962–73.
5. Sulkowski MS, Cooper C, Hunyady B, et al. Management of adverse effects of Peg-IFN and ribavirin therapy for hepatitis C. Nat Rev Gastroenterol Hepatol 2011;8:212–23.
6. Zając M, Muszalska I, Sobczak A, et al. Hepatitis C - New drugs and treatment prospects. Eur J Med Chem 2019;165: 225–49.
7. ElHefnawi MM, Zada S, El-Azab IA. Prediction of prognostic biomarkers for interferon-based therapy to hepatitis C virus patients: a meta-analysis of the NS5A protein in subtypes 1a, 1b, and 3a. Virol J 2010;7:130.
8. Aghemo A, Degasperi E, Colombo M. Directly acting antivirals for the treatment of chronic hepatitis C: unresolved topics from registration trials. Dig Liver Dis 2013;45:1–7.
9. Hofmann WP, Chung TL, Osbahr C, et al. Impact of ribavirin on HCV replicon RNA decline during treatment with interferon-alpha and the protease inhibitors boceprevir or telaprevir. Antivir Ther 2011;16:695–704.
10. Chou TC. Theoretical basis, experimental design, and computerized simulation of synergism and antagonism in drug combination studies. Pharmacol Rev 2006;58:621–81.
11. Windisch MP, Kim HY, Yang J, et al. Compounds for treating viral infections. US Patent 9,809,602 B2. 2017.
12. Kong L, Giang E, Nieusma T, et al. Hepatitis C virus E2 envelope glycoprotein core structure. Science 2013;342:1090–4.
13. Glide. Schrödinger Release 2017-3. Available from: http://content.schrodinger.com/Docs/r2017-3/python_api/overview.html [last accessed 15 Jun 2020].
14. Di Maio VC, Cento V, Mirabelli C, et al. Hepatitis C virus genetic variability and the presence of NS5B resistance-associated mutations as natural polymorphisms in selected genotypes could affect the response to NS5B inhibitors. Antimicrob Agents Chemother 2014;58:2781–97.
15. Pollastri MP. Overview on the rule of five. Curr Protoc Pharmacol 2010;Chapter 9:Unit 9.12.
16. Moraca F, Amato J, Ortuso F, et al. Ligand binding to telomeric G-quadruplex DNA investigated by funnel-metadynamics simulations. Proc Natl Acad Sci USA 2017;114: E2136–45.
17. Hung TC, Jassey A, Liu CH, et al. Berberine inhibits hepatitis C virus entry by targeting the viral E2 glycoprotein. Phytomedicine 2019;53:62–9.
18. Banda DH, Perin PM, Brown RJP, et al. A central hydrophobic E1 region controls the pH range of hepatitis C virus membrane fusion and susceptibility to fusion inhibitors. J Hepatol 2019;70:1082–92.
19. Ma CD, Imamura M, Talley DC, et al. Fluoxazolevir inhibits hepatitis C virus infection in humanized chimeric mice by blocking viral membrane fusion. Nat Microbiol 2020;5: 1532–41.
20. Hu Z, Rolt A, Hu X, et al. Chlorcyclizine inhibits viral fusion of hepatitis C virus entry by directly targeting HCV envelope glycoprotein 1. Cell Chem Biol 2020;27:780–92.e5.
21. Tong Y, Lavillette D, Li Q, et al. Role of hepatitis C virus envelope glycoprotein E1 in virus entry and assembly. Front Immunol 2018;9:1411.